

# Free energy landscape with two barriers and a transient intermediate state determining the unfolding and folding dynamics of cold shock protein

**Haiyan Hong**

Xiamen University

**Zilong Guo**

Xiamen University

**Hao Sun**

Xiamen University

**Ping Yu**

Xiamen University

**Huanhuan Su**

Xiamen University

**Xuening Ma**

Xiamen University

**Hu Chen** (✉ [chenhu@xmu.edu.cn](mailto:chenhu@xmu.edu.cn))

Xiamen University <https://orcid.org/0000-0002-5958-9361>

---

## Article

**Keywords:** cold shock protein (Csp), protein folding, atomic force microscopy (AFM)

**Posted Date:** April 29th, 2021

**DOI:** <https://doi.org/10.21203/rs.3.rs-449394/v1>

**License:**  This work is licensed under a Creative Commons Attribution 4.0 International License.

[Read Full License](#)

---

# Free energy landscape with two barriers and a transient intermediate state determining the unfolding and folding dynamics of cold shock protein

Haiyan Hong<sup>1#</sup>, Zilong Guo<sup>1,2#</sup>, Hao Sun<sup>1</sup>, Ping Yu<sup>1</sup>, Huanhuan Su<sup>1</sup>, Xuening Ma<sup>1</sup>, Hu Chen<sup>1,2\*</sup>

<sup>1</sup> Research Institute for Biomimetics and Soft Matter, Fujian Provincial Key Lab for Soft Functional Materials Research, Department of Physics, Xiamen University, Xiamen 361005, China

<sup>2</sup>Center of Biomedical Physics, Wenzhou Institute, University of Chinese Academy of Sciences, Wenzhou, China 325000

# Contributed equally to this work

E-mail: [chenhu@xmu.edu.cn](mailto:chenhu@xmu.edu.cn)

## Abstract

Cold shock protein (Csp) is a typical two-state folding model protein which has been widely studied by biochemistry and single molecule techniques. Recently two-state property of Csp was confirmed by atomic force microscopy (AFM) through direct pulling measurement, while several long-lifetime intermediate states were found by force-clamp AFM. We systematically studied force-dependent folding and unfolding dynamics of Csp using magnetic tweezers with intrinsic constant force capability. We found that Csp mostly folds and unfolds with a single step over force range from 5 pN to 50 pN, and the unfolding rates show different force sensitivities at forces below and above ~8 pN, which determines a free energy landscape with two barriers and a transient intermediate between them along one transition pathway. Our results provide a new insight on protein folding mechanism of two-state proteins.

## Introduction

Most small single domain proteins fold to unique three-dimensional structure, and the thermodynamics of protein folding and unfolding can be described by

two-state model with highly populated native state and unfolded state only<sup>1,2</sup>. But the detailed mechanism of protein folding/unfolding, such as transition pathway, properties of transition state, and existence of intermediate states, needs further study by newly developed highly sensitive techniques. Theoretically, funnel-shaped free energy landscape with native state at the bottom provides a general picture of proteins folding<sup>3,4</sup>. Transition state separates native state and unfolded state by an energy barrier. Intermediate states are local traps on free energy landscape. Transition pathway connects unfolded state, native state, and possible intermediate states through transition states between them<sup>5</sup>.

Single molecular manipulation techniques apply force to tilt the free energy landscape, and record the conformation transition process of single protein through extension and force signals<sup>6</sup>. Force-dependent transition rate and detection of short-lived intermediate states provide hints to study the complex free-energy landscape of proteins<sup>7</sup>. Cold shock protein B (Csp) from *Thermotoga maritima* is a model protein to study protein folding dynamics with a single peptide chain of 66 amino acids. Csp has a highly conserved single domain structure which can interact with single stranded DNA or RNA<sup>8,9</sup>. Csp functions as nucleic acid chaperons to prevent the formation of DNA/RNA secondary structures at low temperature<sup>10</sup>. Previous bulk experiment and single molecular fluorescence experiment both suggested that Csp is a typical two-state model protein<sup>11-13</sup>. Single-molecule force spectroscopy by atomic force microscope (AFM) measured force-induced unfolding of Csp at constant pulling speeds from 100 nm s<sup>-1</sup> to 2000 nm s<sup>-1</sup>. Single-step unfolding signal of Csp is consistent with two-state model, and pulling-speed-dependent unfolding forces gave unfolding distance  $x_u = 0.49$  nm<sup>14</sup>. At this pulling speed range, average unfolding force is between 75 pN and 90 pN, and the observed unfolding events happen at forces from ~50 pN to ~150 pN. Therefore, under mechanical conditions of both zero force and high force, Csp shows two-state behavior.

Recently, Force-clamp AFM works was used to stretch Csp and record extension time course<sup>15</sup>. Csp was found to unfold through multiple heterogeneous pathways with long-lived intermediate states (lifetime of seconds) at moderate force range from 20 to 80 pN. Unfolding steps with size smaller than expected unfolding step of whole Csp provides direct evidence of

stable intermediate state during Csp unfolding. Molecular dynamic simulation at 200 pN gave unfolding pathways with intermediate state whose lifetime is from several nano-seconds (ns) to tens of ns<sup>15</sup>. Additional simulation based on coarse-grained model<sup>16</sup> also found some intermediate state at low forces of 5-20 pN. But the lifetime of intermediate state is still at time scale of ns. Therefore, there are great discrepancy between force-clamp AFM experiment and simulations according to the lifetime of intermediate states. Single molecule manipulation techniques like AFM and optical tweezers connect an effective Hooke spring to the tethered biomolecule. Therefore, realization of constant force relies on a feedback system. As feedback system usually has finite response time, it might lead errors in measurement of fast dynamic process. Comparing to force feedback system, passive force-clamp mode and constant-trap-position mode are more recommended in optical tweezers.<sup>17</sup>

Magnetic tweezers can maintain stable constant force over long time without any sophisticated force feedback system.<sup>18,19</sup> Here, we report the full-scale study of force-dependent folding and unfolding dynamics of Csp under constant forces using magnetic tweezers. At forces close to critical force of  $\sim 6.6 \pm 0.2$  pN, equilibrium folding and unfolding dynamics gives folding free energy of  $\sim 12.2 \pm 0.8 k_B T$ . At forces up to 50 pN, unfolding rate were measured by force jump experiment. We did not observe intermediate state during both folding and unfolding processes if the measurement was done in three hours after sample preparation. We found that unfolding distance  $x_u$  at forces smaller than 8 pN is much larger than that at large forces. Free energy landscape with two barriers and a transient intermediate state is constructed based on the experimental result.

## Results

### Force-dependent unfolding of Csp measured at constant loading rates.

We tethered the protein of Csp with I27<sub>2</sub> on both flanks through a C-terminus SpyTag attached to the glass surface coated with SpyCatcher and an N-terminus biotin attached to a streptavidin-coated paramagnetic bead M270 (Fig. 1a)<sup>20</sup>. To determine the extension trajectory of Csp during the force-dependent unfolding and folding processes, we increased force from  $\sim 1.2$  pN to  $\sim 25$  pN at

a loading rate of  $1 \text{ pN s}^{-1}$ . An unfolding event was observed at  $\sim 16.6 \text{ pN}$  with a single step of  $\sim 16.5 \text{ nm}$ . After arriving at  $25 \text{ pN}$ , we decreased force to  $1.2 \text{ pN}$  with a loading rate of  $-1 \text{ pN s}^{-1}$ , a refolding step was recorded at  $\sim 4.7 \text{ pN}$  with a single step of  $\sim 8.7 \text{ nm}$  (Fig. 1b). The tether was held for 30 seconds to make sure the protein folds to its original native state. Then force was increased at the same loading rate to  $80 \text{ pN}$ . Besides the unfolding step of Csp, four unfolding steps of I27 with step size  $\sim 25 \text{ nm}$  were observed at force of  $\sim 80 \text{ pN}$ , which confirms that a single target protein is stretched. In force ramp experiments, almost all Csp unfolded events present a single step without long lifetime intermediates, which is consistent with a standard two-state model.

To get enough statistical data of Csp unfolding, multiple stretching cycles were done at the same loading rate. Unfolding force distribution  $P(f)$  at loading rate of  $0.4 \text{ pN s}^{-1}$  was obtained from 81 unfolding events. The average unfolding force is about  $\sim 13.4 \text{ pN}$  which is close to the peak force of this distribution. We suppose that force-dependent unfolding rates follow Bell's model<sup>21</sup> (Supplementary Eq. (1)). Fitting of the obtained unfolding force distribution with Supplementary Eq. (2) gives  $k_u^0 = 0.005 \text{ s}^{-1}$  and  $x_u = 0.97 \text{ nm}$  (Fig. 1c) which is bigger than the result  $0.49 \text{ nm}$  from AFM experiment<sup>14,22</sup>. The corresponding folding force distribution at loading rate of  $0.4 \text{ pN s}^{-1}$  was obtained from 66 folding events. The average folding force is about  $\sim 6.1 \text{ pN}$  which is also close to the peak force of this distribution. Fitting of the obtained folding force distribution with Supplementary Eq. (3) gives  $k_f^0 = 6.4 \times 10^7 \text{ s}^{-1}$  and  $x_f = 12.2 \text{ nm}$  (Fig. 1d)<sup>23,24</sup>. To obtain more accurate force-dependent unfolding property of Csp, we stretched protein Csp at different loading rates from  $0.2 \text{ pN s}^{-1}$  to  $6.0 \text{ pN s}^{-1}$ . Average unfolding force is almost a linear function of logarithm of loading rate (Fig. 1e). Fitting with Supplementary Eq. (4) gives  $k_u^0 = 0.002 \text{ s}^{-1}$  and  $x_u = 1.32 \text{ nm}$ .

The obtained fitting parameters, especially  $x_u$ , show large discrepancy between the above two measurements. Additionally, the obtained  $x_u$  is bigger than previous results by AFM<sup>14</sup>. Therefore, we suspect that force-dependent unfolding rates cannot be described by Bell's model. Theoretically model-independent unfolding rate can be obtained from unfolding force distribution  $P(f)$ , but it requires large amount of data to give an accurate  $P(f)$ <sup>25</sup>.

**Constant force measurement.** Taking advantage of intrinsic constant force capability of magnetic tweezers, we directly measure force response of Csp to constant forces. Based on previous constant loading rate measurement, we know unfolding force of Csp is about 16 pN and the folding occurs at about 5 pN. The critical force at which Csp folds and unfolds with the same rates must be between these two forces. we found that both folding and unfolding transitions of Csp can be observed at constant forces from 5 pN to 7.5 pN. The extension time courses at 5.5, 6.3 and 7 pN are shown in Fig. 2a as examples. The right panel shows the Gaussian fitting of the relative frequency histogram of the smoothed extension with two peaks corresponding to the native and the unfolded states of Csp, respectively. We did the equilibrium measurements for about one hour, and no intermediate state with extension between native state and unfolded state was found. Unfolding and folding probability as a function of time are obtained from cumulative distribution of lifetime of native state and unfolded state, respectively. The exponential fitting gives corresponding  $k_u$  and  $k_f$  at each force (Fig. 2b, 2c). Folding and unfolding probability of Csp at different constant forces are obtained from the bimodal Gaussian fitting of extension (Fig. 2d), which can be fitted with Supplementary Eq. (8) and Eq. (9). Four independent measurements give  $f_c = 6.6 \pm 0.2$  pN and  $\Delta x = 14 \pm 1$  nm which is consistent with the recorded step size (Supplementary Fig. 1).

In order to explore the unfolding rate at higher force range, we did the force jump experiment from 10 pN to 50 pN (Fig. 3). Firstly, we hold the protein at force 1 pN and changed force to various high values abruptly to record unfolding step of Csp. After observing unfolding step of Csp, we decreased force to 1 pN and kept force of 1 pN for 20 sec to make Csp fold to native state. Then another cycle of force jump experiment can be done. Fig. 3 shows three cycles at each force, and the upper traces show zoom-in of unfolding events at each force. Unfolding of Csp happened in one single step, and no intermediate state was detected if experiment was finished in three hours. From waiting time before unfolding at each force, unfolding rates are determined with the same exponential fitting method shown in Fig. 2b.

Force-dependent unfolding rate and folding rate obtained from both equilibrium measurement and force-jump measurement are summarized in Fig. 4a and 4b. We found that the force-dependent unfolding rate from 5 pN to 50

pN cannot be described using Bell's model. The data points of unfolding rates are roughly on two linear lines with distinct slopes. The unfolding rates from 10 to 50 pN can be fitted with bell's model with fitting parameters  $k_{u,1}^0 = (2.8 \pm 0.9) \times 10^{-2} \text{ s}^{-1}$  and  $x_{u,1} = 0.53 \pm 0.03 \text{ nm}$ , which is consistent to the result from AFM experiment<sup>14</sup>. Fitting of unfolding rate from 5 pN to 7 pN provides a zero-force unfolding rate  $k_{u,2}^0 = (4.2 \pm 1.8) \times 10^{-4} \text{ s}^{-1}$  and different unfolding distance  $x_{u,2} = 2.9 \pm 0.3 \text{ nm}$ , which is about 5 times bigger than  $x_{u,1}$ .

As unfolding rates in force range of 10-50 pN and 5-7 pN are obtained from force-jump experiment and equilibrium measurement, respectively, we suspect that the different slopes of fitting lines are due to different methods of measurement. Then we did force-jump measurement from 5 pN to 50 pN and obtained similar results, which proves that the measured unfolding rates are not affected by different experimental strategies (Supplementary Fig. 2). The folding rate obtained from the equilibrium measurement decreases as force increases. Comparing to unfolding rate, the folding rate is much more sensitive to force. The measured force-extension curves of unfolded Csp can be well described by WLC model with a contour length of  $L = 26.0 \pm 0.3 \text{ nm}$  and a persistence length of  $A = 0.80 \pm 0.04 \text{ nm}$  (Supplementary Fig. 3 and Eq. (5-6)). We suppose that the folding transition state is the same as the unfolding transition state in force range of 5-7 pN, then folding transition state has a size of  $l_0 = 4.2 \text{ nm}$ . Then the force-dependent folding rates can be fitted with Supplementary Eq. (11) with a zero-force folding rate  $k_f^0 = 400 \pm 100 \text{ s}^{-1}$  (blue solid curve in Fig. 4a and 4b).

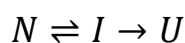
Based on the force-dependent unfolding and folding rates, we can get the force dependent folding free energy  $\Delta G(f)$  according to Supplementary Eq. (10). Then we can calculate the zero-force protein folding free energy using the Supplementary Eq. (7). Independent measurements give  $\Delta G(0) = 12.2 \pm 0.8 k_B T$ .

**Free energy landscape revealed by two different unfolding transition distance.** The distance between N-terminus and C-terminus is 1.32 nm of Csp in the crystal structure. The slopes of the two fitting lines of unfolding rates gives distinct unfolding distances  $x_{u,1} = 0.53 \text{ nm}$  and  $x_{u,2} = 2.9 \text{ nm}$ , which imply that there are two transition states (TS) located at N-C distances of 1.85 nm (for

TS1) and 4.2 nm (for TS2), respectively (Fig. 4c). The size of unfolded state can be estimated as ~6 nm based on free-joint chain model of polypeptide.

If we set the intrinsic unfolding rate<sup>26</sup> of Csp as  $\sim 10^6 \text{ s}^{-1}$ , then the energy barriers can be estimated to be  $17.3 k_B T$  (TS1) and  $21.6 k_B T$  (TS2). Between TS1 and TS2, we speculate that there exists an intermediate state (I), although it was not observed in our experiment directly. With free energy of native state as reference, a free energy landscape is constructed along reaction coordinate of N-C distance based on folding free energy, barrier heights and locations of TS1 and TS2 (Fig. 4).

Based on the free energy landscape, we can modify the two-state model by incorporating the intermediate state I between N and U states (NIU model):



We found that the unfolding rate is not sensitive to location of state I along the unfolding pathway (Fig. 4c). As we cannot detect state I directly in recorded time course of extension, state I must be not very stable. We suppose that state I has free energy  $\sim 14 k_B T$  and located at position in the middle of TS1 and TS2, the force-dependent unfolding rates can be fitted with analytical equations of NIU model derived by Pierse and Dudko<sup>27</sup> (Fig. 4a, Supplementary Note 2). Interdependence between parameters is given in Supplementary Fig. 5.

## Discussion

In summary, force-dependent unfolding and folding rate of Csp at a force range from 5 pN to 50 pN were measured directly by magnetic tweezers, especially the force-dependent folding rate which is not measured before. The equilibrium measurement at 5-7 pN directly determines critical force of 6.6 pN and zero force folding free energy of Csp  $\sim 12.2 k_B T$ .

For most protein tethers, we didn't record a direct intermediate state in multiple cycles of constant loading rate and force jump experiment. This is in contrast to previous force-clamp AFM measurement which detected several long-lifetime intermediate states during the unfolding process<sup>15</sup>. Occasionally, after several hours measurement, multi-step unfolding events start to be

observed (Supplementary Fig. 4). One possibility is that the protein was injured at some unknown position during such long-time measurement.

We found that force-dependent unfolding rate cannot be fitted with Bell's model. Unfolding of Csp is more sensitive to force when force is smaller than 8 pN, and less sensitive to force at force range greater than 8 pN. A similar phenomenon has been found in GB1 protein<sup>28</sup>. As shown in Fig. 4c, TS1 with  $x_{u,1} = 0.53$  nm determines the flexibility of Csp native state. Comparing to I27 and GB1, native state of Csp is more flexible, which may be the structural basis for its function to interact with single stranded DNA or RNA as a nucleic acid chaperon<sup>14,29</sup>.

Because we cannot directly record the transient intermediate state I between the two transition states TS1 and TS2 from extension steps of folding and unfolding transitions, it indicates that I state must have a relatively high free energy. This intermediate state might be the molten globule state proposed in traditional protein folding theory<sup>30</sup>. Then TS2 serves as the general barrier between the molten globule state and unfolded polypeptide. As the N-C distance in native state of Csp is only ~1.3 nm, TS2 with size about 4.2 nm can be easily distinguished from TS1.

From the viewpoint of technology capability, our results demonstrate the importance of measurement over large force range which is one advantage of magnetic tweezers. If only force-dependent unfolding rates at forces greater than 10 pN are measured as previous AFM measurements<sup>14,15</sup>, the transition state of TS2 will be ignored. On the other hand, if only equilibrium folding/unfolding dynamics are measured in the vicinity of critical force 6.6 pN, TS1 cannot be detected. Therefore, measurement of folding and unfolding rates over a large force range is critical to construct the full free energy landscape of proteins, and magnetic tweezers are most suitable to accomplish this measurement among single molecule manipulation techniques.

## Methods

**Cloning and protein expression.** The recombinant protein construct 6xHis-AviTag-I27<sub>2</sub>-Csp-I27<sub>2</sub>-SpyTag was made by inserting the DNA sequence of Csp (synthesized by GenScript Biotech) into the vector pET151-I27<sub>4</sub>, which had two

Titin-I27 domains on each side of multiple cloning site. To generate biotinylated protein, plasmids of pET151-6xHis-AviTag-I27<sub>2</sub>-Csp-I27<sub>2</sub>-SpyTag and pBirA (Biotin ligase expression plasmid) were transformed into the E. coli strain BL21 (DE3). Selected transformants on LB plates were cultured in LB medium (supplemented with chloramphenicol, ampicillin, D-biotin) at 310 K until the optical density (OD) of the Bacterial cell reached 0.6. Protein expression was induced with 0.5 mM isopropyl  $\beta$ -D-thiogalactopyranoside (IPTG) for 12 h at 298 K. The cells were harvested by centrifugation and lysed by sonication in a buffer (50 mM Tris, 500 mM NaCl, 10 % glycerol, 5 mM imidazole, 5 mM 2-mercaptoethanol, pH 8.0). The target recombinant protein was purified by using Ni-NTA Sefinose (TM) Resin (Sangon Biotech) and Superdex 200 (GE Healthcare,) according to the manufacturer's protocol. The protein was snap frozen in liquid nitrogen and stored at 193 K.

**Single-molecule magnetic tweezers measurements.** The target protein was coupled between the glass coverslip of a laminar flow chamber and a 2.8  $\mu$ m diameter paramagnetic bead (Dynabeads M270, Invitrogen) (Fig. 1a). Coverslips were cleaned in an ultrasonic cleaner in 5 % Decon90 detergent, then were treated by oxygen plasma cleaner for 10 min. Cleaned coverslips were incubated in solution of 1% 3-aminopropyltriethoxysilane (APTES, cat. A3648, Sigma) in methanol for 1 h and rinsed by methanol. Flow chambers were assembled by adding parafilm as spacer between the APTES-coated coverslip and another cleaned coverslip. Amino functionalized microspheres (Polybead cat.417145, Polysciences) with 3  $\mu$ m diameter were added and incubated for 20 min in the chamber. They stuck on surface and was used as reference to eliminate spatial drift during experiments. Then SpyCatcher protein was immobilized on to the coverslip after 1% Sulfo-SMCC (SE 247420, Thermo Science) was incubated for 20 min in the chamber. The chamber was blocked by 1% BSA in 1xPBS over night at room temperature. Protein with N-terminus AviTag and C-terminus SpyTag was flowed into chamber and incubated for 25 min, then streptavidin-coated paramagnetic beads M270 were flowed into the chamber to form tether.

Home-made magnetic tweezers were used to apply stretching force to Csp protein tether to study its force-dependent folding and unfolding dynamics.

Constant loading rates between  $0.25 \text{ pN s}^{-1}$  and  $6 \text{ pN s}^{-1}$  were used by moving magnets with different speeds. Force jump experiments were done by moving magnets rapidly in less than 0.15 sec. Details of magnetic tweezers design can be referenced to our previous publication<sup>19</sup>.

### **Data availability**

The authors declare that all data supporting the findings of this study are available within the article and its supplementary information files.

### **Acknowledgements**

This work was supported by the National Natural Science Foundation of China (Grant No. 11874309, 11474237) and 111 project (B16029).

### **Author contributions**

H.H. and Z.G. designed and did the experiments and analyzed the data, contributed equally to this work. H.S., P.Y., H.S., and X.M. made the channels and some data collection. H.C. directed the project. H.C. and H.H. wrote the paper.

### **Additional information**

**Supplementary information** Theoretical modeling with Supplementary Eqs. 1-15 and fitting parameters; Supplementary Figs. 1-5.

**Competing interests:** The authors declare no competing interests.

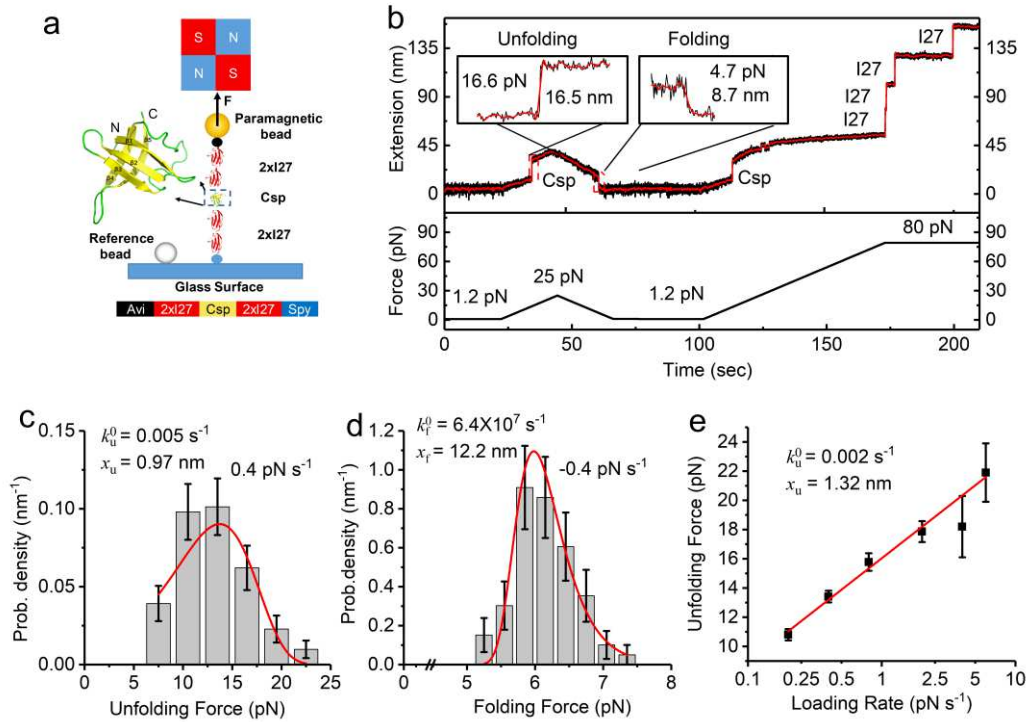


**Fig. 1 Force-dependent unfolding and refolding of Csp measured by magnetic tweezers at constant loading rates.** **a** Sketch of magnetic tweezers pulling protein construct of 2xI27-Csp-2xI27 with the AviTag at N-terminus attached to a streptavidin coated paramagnetic bead and SpyTag at C-terminus attached to the glass surface coated with Spycatcher. Zoomed in figure shows structure of Csp. **b** Extension time course of 2xI27-Csp-2xI27 in a force cycle at a loading rates of  $\pm 1 \text{ pN s}^{-1}$  from 1.2 pN to 25 pN, an unfolding step and a refolding step were observed at  $\sim 16.6 \text{ pN}$  and  $\sim 4.7 \text{ pN}$ , respectively. After waiting for 30 second at 1.2 pN, force was increased at loading rate of  $1 \text{ pN s}^{-1}$  to 80 pN, additional four unfolding steps I27 were observed after unfolding of Csp. Raw data were recorded at 200 Hz (black) and smoothed in time window of one second (red). **c** Unfolding force distribution at constant loading rate of  $0.4 \text{ pN s}^{-1}$  were obtained from 81 unfolding events. The fitting of unfolding probability density with Supplementary Eq. (2) gives a  $k_u^0 = 0.005 \text{ s}^{-1}$  and  $x_u = 0.97 \text{ nm}$ . **d** Folding force distribution at constant loading rate of  $0.4 \text{ pN s}^{-1}$  were obtained from 66 folding events. The fitting of folding probability density with Supplementary Eq. (3) gives a  $k_f^0 = 6.4 \times 10^7 \text{ s}^{-1}$  and  $x_f = 12.2 \text{ nm}$ . **e** The average unfolding forces were obtained at loading rate from  $0.2 \text{ pN s}^{-1}$  to  $6 \text{ pN s}^{-1}$ . Linear fitting with Supplementary Eq. (4) gives a  $k_u^0 = 0.002 \text{ s}^{-1}$  and  $x_u = 1.32 \text{ nm}$ .

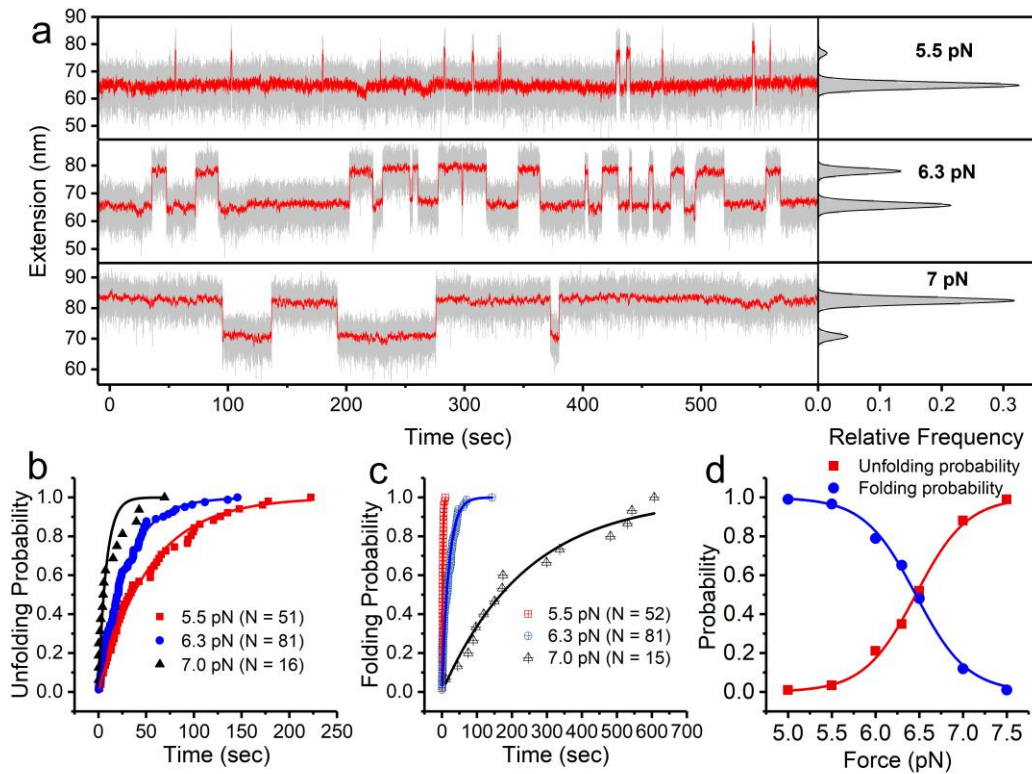


**Fig. 2 Equilibrium measurement of Csp at various constant forces. a** Extension time course of Csp at three constant forces of 5.5 pN, 6.3 pN, 7 pN were recorded for 600 seconds. Corresponding relative frequency distributions of the extensions were shown in right panel and fitted by Gauss functions. Raw data were recorded at 200 Hz (gray) and smoothed over five-second time window (red). **b, c** The Unfolding and folding probability of Csp at the three constant forces. Solid lines show exponential fitting curves to determine  $k_u$  and  $k_f$  of Csp. **d** The force-dependent folding/unfolding probability data points were fitted with Supplementary Eqs. (8-9).

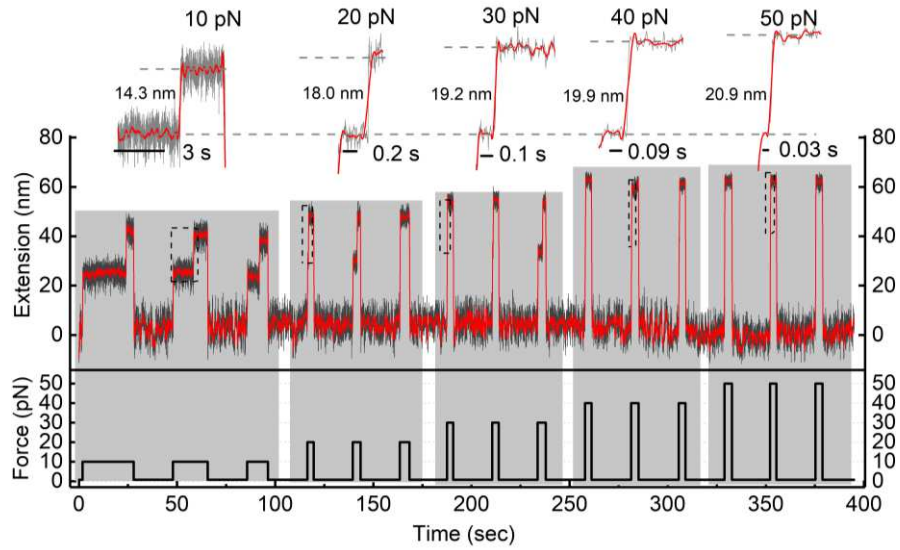


**Fig. 3 Unfolding process of Csp at various constant forces measured in force-jump experiment.** Unfolding steps were recorded after force jumped from 1 pN to various high forces (10, 20, 30, 40 and 50 pN) on the same protein tether. Before each measurement, force of 1 pN was applied for 20 sec to make Csp protein folds to its native state. The upper traces show zoom-in of unfolding events at each force. Red curve shows smoothed extension over one-second time window.

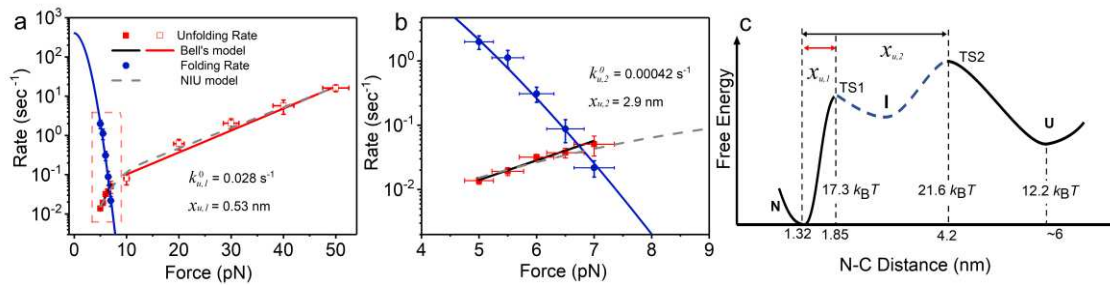


**Fig. 4 Force-dependent folding rates and unfolding rates and free energy landscape of Csp.** **a, b** Unfolding and folding rates of Csp measured by equilibrium constant force experiment (solid symbol) and force-jump experiment (open symbol). The unfolding rates were fitted using Bell's model at force range from 5 to 7 pN (black line) and from 10 to 50 pN (red line) separately, which gives us two different  $x_u$ :  $x_{u,1} = 0.53 \pm 0.03 \text{ nm}$ ,  $x_{u,2} = 2.9 \pm 0.3 \text{ nm}$ , and corresponding parameters  $k_{u,1}^0 = (2.8 \pm 0.9) \times 10^{-2} \text{ s}^{-1}$ ,  $k_{u,2}^0 = (4.2 \pm 1.8) \times 10^{-4} \text{ s}^{-1}$ , respectively. Nonlinear force dependent unfolding rates at force range 5–50 pN are fitted with a hidden intermediate state using NIU model (gray dashed line, Supplementary Eqs. 12-16). The folding rates were fitted using Arrhenius' law (solid blue line, Supplementary Eq. (11) and  $k_f^0 = 400 \pm 100 \text{ s}^{-1}$ . **c** Free energy landscape of Csp at zero force is plotted as a function of N-C distance. With free energy of N as a reference, free energy of U is obtained by Supplementary Eq. (7). Free energy of TS1 (TS2) is calculated from fitting parameters of Bell's mode  $k_{u,1}^0$  ( $k_{u,2}^0$ ) based on equation  $k_u^0 = k^* \exp(-\Delta G^\ddagger)$  where the pre-factor  $k^* = 10^6 \text{ s}^{-1}$ . An intermediate state located between TS1 and TS2 might exist but is not stable enough to be recorded in experiments.

## References

- 1 Finkelstein, A. V. 50+ years of protein folding. *Biochemistry* **83**, S3-S18 (2018).
- 2 Jackson, S. E. How do small single-domain proteins fold? *Fold. Des.* **3**, R81-R91 (1998).
- 3 Wolynes, P. G., Onuchic, J. N. & Thirumalai, D. Navigating the folding routes. *Science* **267**, 1619-1620 (1995).
- 4 Finkelstein, A. V. *et al.* There and back again: Two views on the protein folding puzzle. *Phys. Life Rev.* **21**, 56-71 (2017).
- 5 Kim, P. S. & Baldwin, R. L. Specific intermediates in the folding reactions of small proteins and the mechanism of protein folding. *Annu. Rev. Biochem.* **51**, 459-489 (1982).
- 6 Neuman, K. C. & Nagy, A. Single-molecule force spectroscopy: optical tweezers, magnetic tweezers and atomic force microscopy. *Nat. Methods* **5**, 491-505 (2008).
- 7 Oliveberg, M. & Wolynes, P. G. The experimental survey of protein-folding energy landscapes. *Q. Rev. Biophys.* **38**, 245-288 (2005).
- 8 Horn, G., Hofweber, R., Kremer, W. & Kalbitzer, H. R. Structure and function of bacterial cold shock proteins. *Cell. Mol. Life Sci.* **64**, 1457-1470 (2007).
- 9 Max, K. E., Zeeb, M., Bienert, R., Balbach, J. & Heinemann, U. T-rich DNA single strands bind to a preformed site on the bacterial cold shock protein Bs-CspB. *J. Mol. Biol.* **360**, 702-714 (2006).
- 10 Keto-Timonen, R. *et al.* Cold shock proteins: A minireview with special emphasis on Csp-family of enteropathogenic yersinia. *Front. Microbiol.* **7**, 1151 (2016).
- 11 Perl, D. *et al.* Conservation of rapid two-state folding in mesophilic, thermophilic and hyperthermophilic cold shock proteins. *Nat. Struct. Biol.* **5**, 229-235 (1998).
- 12 Schuler, B., Lipman, E. A. & Eaton, W. A. Probing the free-energy surface for protein folding with single-molecule fluorescence spectroscopy. *Nature* **419**, 743-747 (2002).
- 13 Rhoades, E., Cohen, M., Schuler, B. & Haran, G. Two-state folding observed in individual protein molecules. *J. Am. Chem. Soc.* **126**, 14686-14687 (2004).
- 14 Hoffmann, T., Tych, K. M., Brockwell, D. J. & Dougan, L. Single-molecule force spectroscopy identifies a small cold shock protein as being mechanically robust. *J. Phys. Chem. B* **117**, 1819-1826 (2013).
- 15 Schonfelder, J., Perez-Jimenez, R. & Munoz, V. A simple two-state protein unfolds mechanically via multiple heterogeneous pathways at single-molecule resolution. *Nat. Commun.* **7**, 11777 (2016).
- 16 de Sancho, D. & Best, R. B. Reconciling Intermediates in Mechanical Unfolding Experiments with Two-State Protein Folding in Bulk. *J. Phys. Chem. Lett.* **7**, 3798-3803 (2016).
- 17 Elms, P. J., Chodera, J. D., Bustamante, C. J. & Marqusee, S. Limitations of constant-force-feedback experiments. *Biophys. J.* **103**, 1490-1499 (2012).
- 18 Chen, H. *et al.* Improved high-force magnetic tweezers for stretching and refolding of proteins and short DNA. *Biophys. J.* **100**, 517-523 (2011).
- 19 Chen, H. *et al.* Dynamics of equilibrium folding and unfolding transitions of titin

- immunoglobulin domain under constant forces. *J. Am. Chem. Soc.* **137**, 3540-3546 (2015).
- 20 Zakeri, B. *et al.* Peptide tag forming a rapid covalent bond to a protein, through engineering a bacterial adhesin. *Proc. Natl. Acad. Sci. USA* **109**, E690-697 (2012).
- 21 Bell, G. I. Models for the specific adhesion of cells to cells. *Science* **200**, 618-627 (1978).
- 22 Schlierf, M., Li, H. & Fernandez, J. M. The unfolding kinetics of ubiquitin captured with single-molecule force-clamp techniques. *Proc. Natl. Acad. Sci. USA* **101**, 7299-7304 (2004).
- 23 Strunz, T., Oroszlan, K., Schafer, R. & Guntherodt, H. J. Dynamic force spectroscopy of single DNA molecules. *Proc. Natl. Acad. Sci. USA* **96**, 11277-11282 (1999).
- 24 Sulchek, T. A. *et al.* Dynamic force spectroscopy of parallel individual Mucin1-antibody bonds. *Proc. Natl. Acad. Sci. USA* **102**, 16638-16643 (2005).
- 25 Dudko, O. K., Hummer, G. & Szabo, A. Theory, analysis, and interpretation of single-molecule force spectroscopy experiments. *Proc. Natl. Acad. Sci. USA* **105**, 15755-15760 (2008).
- 26 Best, R. B. & Hummer, G. Diffusive model of protein folding dynamics with Kramers turnover in rate. *Phys. Rev. Lett.* **96**, 228104 (2006).
- 27 Pierse, C. A. & Dudko, O. K. Distinguishing signatures of multipathway conformational transitions. *Phys. Rev. Lett.* **118**, 088101 (2017).
- 28 Guo, Z. *et al.* Hidden Intermediate State and Second Pathway Determining Folding and Unfolding Dynamics of GB1 Protein at Low Forces. *Phys. Rev. Lett.* **125** (2020).
- 29 Gao, X. *et al.* Single-molecule experiments reveal the flexibility of a Per-ARNT-Sim domain and the kinetic partitioning in the unfolding pathway under force. *Biophys. J.* **102**, 2149-2157 (2012).
- 30 Baldwin, R. L. & Rose, G. D. Molten globules, entropy-driven conformational change and protein folding. *Curr. Opin. Struct. Biol.* **23**, 4-10 (2013).

# Figures

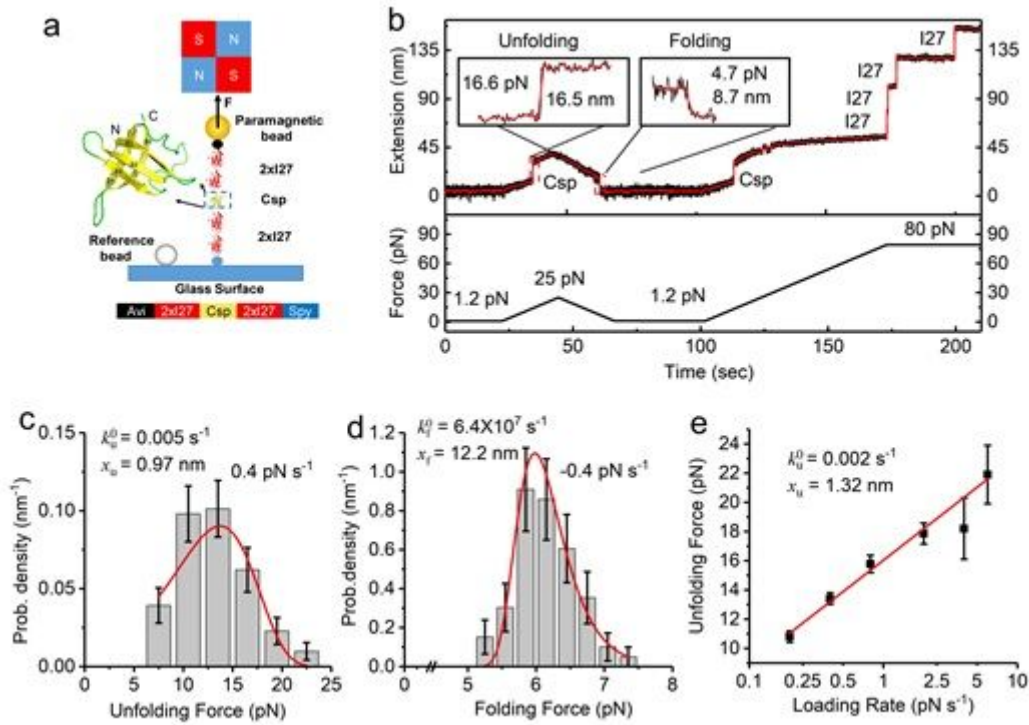
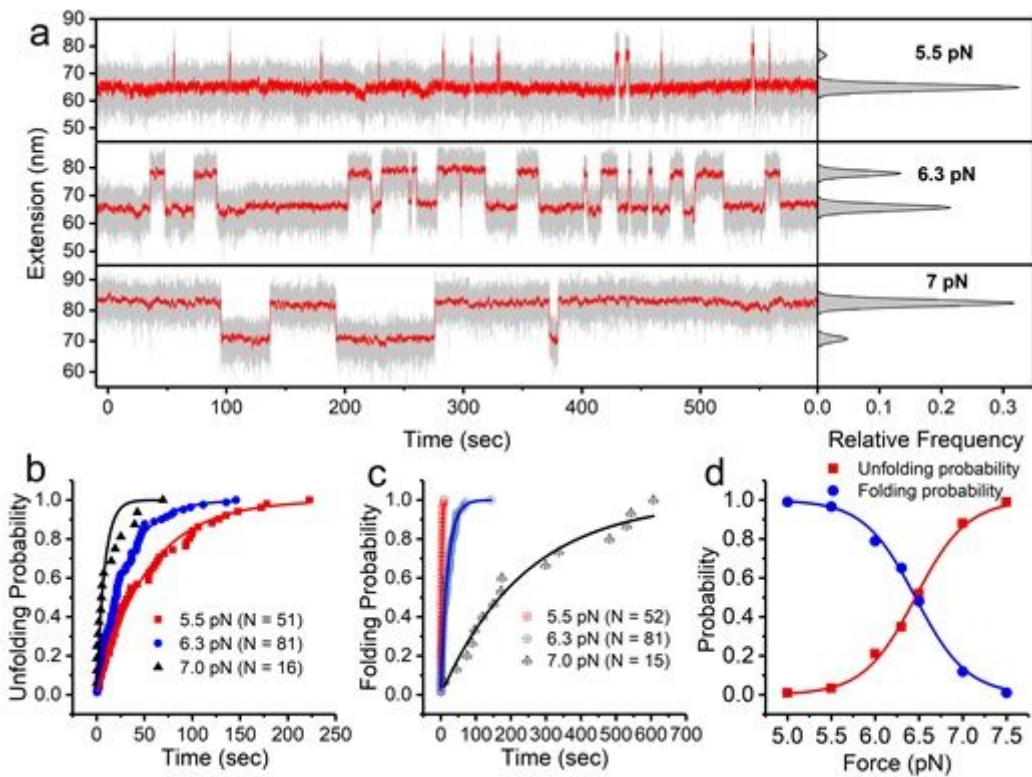


Figure 1

Force-dependent unfolding and refolding of Csp measured by magnetic tweezers at constant loading rates. (see Manuscript file for full figure caption)



**Figure 2**

Equilibrium measurement of Csp at various constant forces. (see Manuscript file for full figure caption)

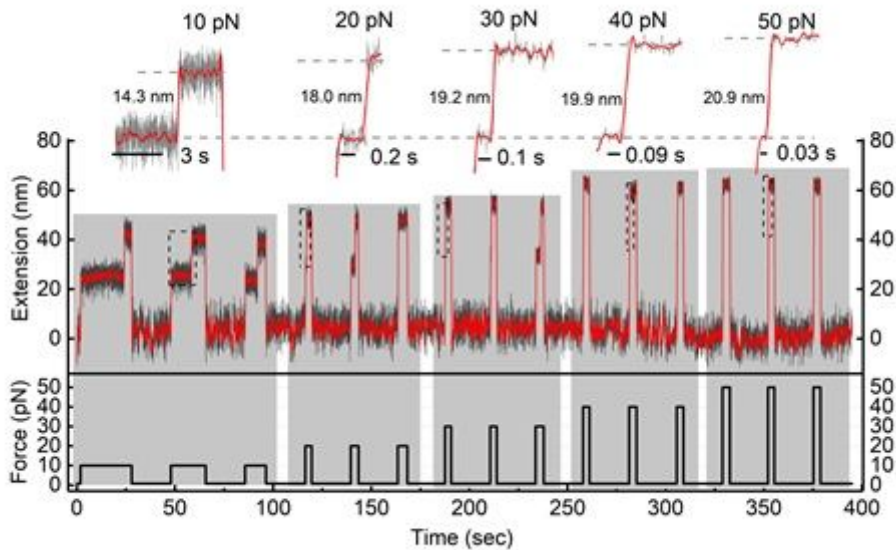


**Figure 3**

Unfolding process of Csp at various constant forces measured in force-jump experiment. (see Manuscript file for full figure caption)

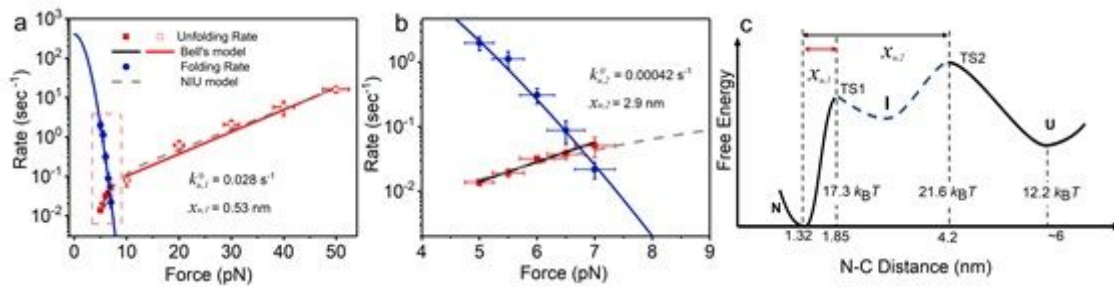


**Figure 4**

Force-dependent folding rates and unfolding rates and free energy landscape of Csp. (see Manuscript file for full figure caption)

## Supplementary Files

This is a list of supplementary files associated with this preprint. Click to download.

- [SlforCsppaper.docx](#)